Materials Science and Technology DOI: 10.1179/1743284714Y.0000000746 (2015)

Computational thermodynamics in electric current metallurgy

R.S. Qin[1] and A. Bhowmik[2]

1. Department of Engineering and Innovation, The Open University, Walton Hall, Milton Keynes MK7 6AA, England

2. DTU National Laboratory for Sustainable Energy, Technical University of Denmark, Frederiksborgvej 399, 4000 Roskilde, Denmark

A priori derivation for the extra free energy caused by the passing electric current in metal is presented. The analytical expression and its discrete format in support of the numerical calculation of thermodynamics in electric current metallurgy have been developed. This enables the calculation of electric current distribution, current-induced temperature distribution and free energy sequence of various phase transitions in multiphase materials. The work is particularly suitable for the study of magnetic materials that contains various magnetic phases. The latter has not been considered in literature. The method has been validated against the analytical solution of current distribution and experimental observation of microstructure evolution. It provides a basis for the design, prediction and implementation of the electric current metallurgy. The applicability of the theory is discussed in the derivations.

Keywords: Electric current metallurgy, Magnetic materials, Thermodynamics

Authors to whom correspondence should be addressed. Email: rongshan.qin@open.ac.uk. Tel.: +44 (0)1958 652 999.

Introduction

Electric current metallurgy utilizes electric current in alloys processing [1]. The system free energy in this situation consists of chemical free energy (G_c), interfacial energy (G_i), strain-stress energy (G_s) and electric current free energy (G_e). G_c can be calculated using Redlich–Kister equation [2]. G_i can be calculated by broken-bond and binding-energy models [3]. G_s can be obtained by the calculation or measurement of strain field [4]. G_e is an extra free energy caused by the electric current. There is an equation in literature that is applicable to the calculation of G_e for the non-magnetic materials [5]. For the magnetic materials, especially for materials containing phases with different values of magnetic permeability, the existing theory is not applicable. Furthermore, the analytical calculation for the current distribution and G_e in the analysis of multiphase alloys is feasible for only a few oversimplified cases [5-7]. Numerical calculation method for this problem has not been developed and discussed systematically. A priory derivation for thermodynamics of electric current metallurgy is desirable. This will not only contribute to the fundamental understanding of the effect of electric current in metallurgy but also to clarify the limitations in application of the theory to the design of the electric current metallurgy. This article serves such purposes.

The extra free energy in electric current metallurgy

For an infinitesimal volume δV inside a metallic material, the conductive electrons are driven to drift toward a direction by the applied electric potential upon the materials. Denote the density of conductive electrons inside the considering volume by ρ_c, electron drift velocity $\vec{v}_d$, local electric field $\vec{E}$ and the local electrophoresis force $\vec{F}_e$, the required work for moving the electrons and generating an infinitesimal displacement, $\delta\vec{s}$, is

$$\delta w = \vec{F}_e \cdot \delta\vec{s} \tag{1}$$

The procedure is supposed to take an infinitesimal time δt. It has $\delta\vec{s} = \vec{v}_d \delta t$ and $\vec{F}_e = \vec{E}\rho_c$ Eq. (1) can be further expressed as

$$\delta w = \left(\vec{E}\rho_c\right)\cdot\left(\vec{v}_d\delta t\right) = \vec{E}\cdot\left(\rho_c\vec{v}_d\right)\delta t = \vec{E}\cdot\vec{j}\,\delta t \tag{2}$$

where $\vec{j}$ is the local electric current density. According to Ampere's Law, $\nabla\times\vec{H} = \vec{j} + \partial\vec{D}/\partial t$, where $\vec{D}$ is electric displacement and $\vec{H}$ is the magnetic field strength. In steady state, one has $\partial\vec{D}/\partial t = 0$ and hence $\nabla\times\vec{H} = \vec{j}$. Substituting this to Eq. (2) leads to

$$\delta w = \vec{E}\cdot\left(\nabla\times\vec{H}\right)\delta t = \nabla\cdot\left(\vec{E}\times\vec{H}\right)\delta t - \vec{H}\cdot\left(\nabla\times\vec{E}\right)\delta t \tag{3}$$

Integration of Eq. (3) throughout the space gives the total work required to drive conductive electrons to drift in a time interval δt. The divergence theorem states

$$\iiint \nabla\cdot\left(\vec{E}\times\vec{H}\right)dV = \oiint\left(\vec{E}\times\vec{H}\right)\cdot d\vec{S} = 0 \tag{4}$$

where $d\vec{S} = \hat{n}dS$ is the surface element and $\hat{n}$ is the normal vector. The integration of Eq. (3) after consideration of Eq. (4) gives

$$\delta W = \iiint \delta w dV = -\iiint\left[\vec{H}\cdot\left(\nabla\times\vec{E}\right)\delta t\right]dV \tag{5}$$

Substituting Faraday's Law $\nabla\times\vec{E} = -\delta\vec{B}/\delta t$ into Eq. (5), one has

$$\delta W = \iiint\left(\vec{H}\cdot\delta\vec{B}\right)dV \tag{6}$$

where $\vec{B}$ is magnetic field. Eq. (6) has a new meaning of the work needed to cause a small change of magnetic field $\delta\vec{B}$. The magnetic field $\vec{B}$ works both to against the electric field that a changing magnetic field creates and to change the magnetization of any material within the magnetic field. For non-dispersive materials this same energy is released when the magnetic field is destroyed so that this energy can be modelled as being stored in the magnetic field. In this case, the free energy is represented as

$$G_e = -\frac{1}{2}\iiint\left(\vec{H}\cdot\vec{B}\right)dV \tag{7}$$

Using $\vec{B} = \nabla\times\vec{A}$, $\vec{H}\cdot\left(\nabla\times\vec{A}\right) = \vec{A}\cdot\left(\nabla\times\vec{H}\right) - \nabla\cdot\left(\vec{H}\times\vec{A}\right)$ and the divergence theorem, Eq. (7) changes into following format

$$G_e = -\frac{1}{2}\iiint\left[\vec{A}\cdot\left(\nabla\times\vec{H}\right)\right]dV = -\frac{1}{2}\iiint\left(\vec{A}\cdot\vec{j}\right)dV \tag{8}$$

where $\vec{A}$ is the vector potential. Eq. (7) and Eq. (8) are two equivalent formats for the calculation of system free energy [8]. By notice that $\vec{j} = 0$ outside the materials, integration of Eq. (8) requires only inside the material. For the tidiness Eq. (8) can be denoted as

$$G_e = -\frac{1}{2}\int_V \vec{A}(r)\cdot\vec{j}(r)dr \tag{9}$$

where r is a position inside the materials. V is the materials volume. One needs to find the solution of vector potential $\vec{A}$. From $\vec{B}=\nabla\times\vec{A}$, one has

$$\nabla\times\vec{B}=\nabla\times\left(\nabla\times\vec{A}\right)=\nabla\left(\nabla\cdot\vec{A}\right)-\nabla^2\vec{A}=-\nabla^2\vec{A} \tag{10}$$

where Coulomb Gauge condition gives $\nabla\left(\nabla\cdot\vec{A}\right)=0$. For linear non-dispersive materials, following equation stands

$$\vec{B}=\mu\vec{H} \tag{11}$$

where μ is the magnetic permeability and is frequency dependent. If there is no magnetic materials around one has $\mu=\mu_0$, where μ_0 is the magnetic permeability in vacuum. At steady state, substituting $\vec{j}=\nabla\times\vec{H}$ to $\nabla\times\vec{B}=\mu\nabla\times\vec{H}$ gives $\nabla\times\vec{B}=\mu\vec{j}$. Eq. (10) is thus changed into a Poisson equation as following

$$\nabla^2\vec{A}=-\mu\vec{j} \tag{12}$$

The general solution of the Poisson equation is

$$\vec{A}(r)=\frac{1}{4\pi}\int_V\frac{\mu(r')\vec{j}(r')}{|r-r'|}dr' \tag{13}$$

where r' is a point in the materials. Substituting Eq. (13) into (9), one has

$$G_e=-\frac{1}{8\pi}\int_V\int_V\frac{\mu(r')\vec{j}(r')\cdot\vec{j}(r)}{|r-r'|}drdr' \tag{14}$$

Eq. (14) is suitable to describe the free energy of multiphase linear non-dispersive materials at a steady state. The phases constituting the materials may have different magnetic permeability. This expression is different from that in literature [5].

Computation of current distribution and free energy

Calculation of Eq. (14) requires the knowledge of current distribution in materials. For some simple cases, e.g. an infinite large matrix containing only one spherical or ellipsoidal inclusions, the analytical solution for the electric current distribution can be derived from Maxwell equations [9]. However, it is not possible to obtain an analytical expression of the electric current distribution in engineering multiphase polycrystalline alloys from solving of Maxwell equations. Numerical calculation of the current distribution at steady state can overcome this difficult.

A continuous material can be discretized into and represented by some nodes and elements. The nodes can be arranged regularly and irregularly. An element linking to node-α and node-γ is called element-αγ. Node-α can connect to β-number of nodes via elements, as illustrated schematically in Figure 1. In the low-frequency limit where the wavelengths of electromagnetic radiation are very large compared to the materials dimension, Kirchhoff's circuit laws satisfied, which is

$$\sum_{\gamma=1}^{\beta} I_{\alpha\gamma} = 0 \tag{15}$$

where $I_{\alpha\gamma}$ represents the electric current in the element-αγ. The current density in the element can be obtained by $j_{\alpha\gamma} = I_{\alpha\gamma} / S_{\alpha\gamma}$ with $S_{\alpha\gamma}$ denotes the cross section area of element-αγ. The low-frequency limit is normally satisfied in engineering metallurgical processing, e.g. 300 Hz alternating current has a wavelength of 1000 km which is much large than a typical alloy product. Eq. (15) is, however, accurate for the application of direct current.

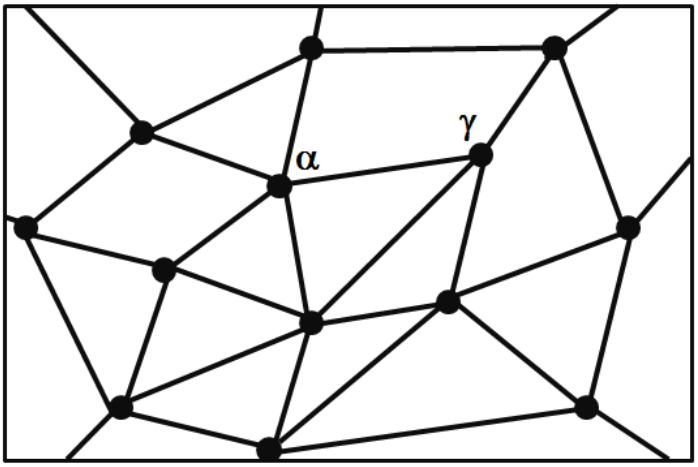

Fig. 1 Schematical diagram of nodes (α, γ, …) and elements (the bar from α to γ).

Denoting the electric potential at node-α by ϕ_α and the electrical conductance of element-αγ by $\sigma_{\alpha\gamma}$, Eq. (15) is represented as

$$\sum_{\gamma=1}^{\beta} \left(\phi_\gamma - \phi_\alpha\right)\sigma_{\alpha\gamma} = 0 \tag{16}$$

One has

$$\phi_\alpha = \sum_{\gamma=1}^{\beta} \phi_\gamma \sigma_{\alpha\gamma} / \sum_{\gamma=1}^{\beta} \sigma_{\alpha\gamma} \tag{17}$$

Eq. (17) is the governing equation for numerical calculation of electric potential distribution, and is particularly suitable to be solved by discrete numerical methods such as the relaxation method. Once the electric potential distribution ϕ_α at the steady state is calculated, the current density distribution can be obtained by

$$j_{\alpha\gamma} = \left(\phi_\alpha - \phi_\gamma\right)\sigma_{\alpha\gamma} / S_{\alpha\gamma} \tag{18}$$

The heating rate due to Ohm heat at element-αγ is obtainable by

$$\dot{T}_{\alpha\gamma} = \left(\phi_\gamma - \phi_\alpha\right)^2 \sigma_{\alpha\gamma} / \left(m_{\alpha\gamma} c_{\alpha\gamma}\right) \tag{19}$$

Where $m_{\alpha\gamma}$ and $c_{\alpha\gamma}$ are mass and specific heat of element-αγ, respectively. The system free energy can be calculated numerically by

$$G_e = -\frac{1}{8\pi} \sum_\alpha \sum_\gamma \frac{\mu(r_\alpha)\vec{j}(r_\alpha) \cdot \vec{j}(r_\gamma) V_\alpha V_\gamma}{\left|r_\alpha - r_\gamma\right|} \tag{20}$$

where V_α and V_γ are the volume of node-α and node-γ, respectively.

Validation against the analytical theory and experimental observation

The analytical solution for the electric current distribution in an infinite large material containing a tiny spherical inclusion is available [5, 6, 9]. Denote the electrical conductivity of matrix by σ_0 and that of the inclusion by σ_n, a schematic illustration for the current distribution for both $\sigma_n > \sigma_0$ and $\sigma_n < \sigma_0$ are reported in literature [9]. Using the relaxation method, the electric current distribution for $\sigma_n < \sigma_0$ has been calculated using the theory presented in the present work. Figure 2 shows the numerical result. The vertical lines in Figure (2) are the electric potential contours. The left side is assigned to higher electrical potential than that of the right side. The perpendicular lines to the electric potential contour lines are the current stream lines. It can be found obviously that the characters on the current streamlines around the spherical inclusions are in good agreement with the analytical solution at $\sigma_n < \sigma_0$. The relationship between current streamlines and electric potential contour lines agrees with the knowledge in electrodynamics.

To validate the theory against the experimental observation, the evolution of the precipitates in a stainless steel at high temperature (above Curie temperature) is selected for the study. It is found experimentally that the precipitates with a composition of Fe-10.45Ni-16.68Cr-2.02Mo (at.%) are formed after high temperature annealing. The matrix is with a composition of Fe-7.78Ni-24.13Cr-6.57Mo (at.%). When the electric current is applied to the alloy at the high temperature annealing, the precipitates dissolve [10].

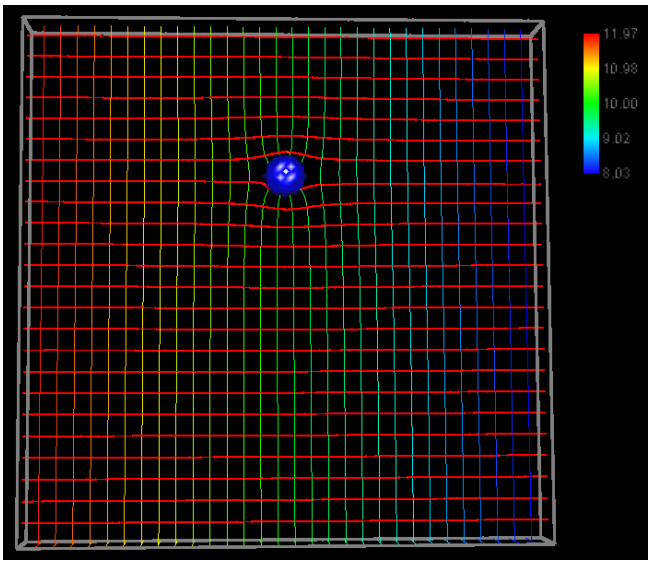

Fig. 2 The distribution of current streamlines in a material containing a spherical inclusion. The vertical lines are electric potential contours. The electrical conductivity of inclusion is smaller than that of the matrix ($\sigma_n < \sigma_0$).

Numerical calculations have been performed on a sample whose dimensions are 2 cm×1 cm×0.8 cm. 100×50×40 cubically arranged nodes are setup for computation. Each node is connected to 6 neighbouring nodes via elements. The length of each element is $\Delta h = 200$ μm. The boundary electric potentials are defined as $U_i = 20$ volts at $x = 0$ and $U_o = 0$ at $x = 2$ cm respectively. The parameters are chosen after reference of real parameters in experimental

processing. The electrical resistivity of a multicomponent phase is calculated using Matthiessen rule [11]

$$\rho = \rho_0(T) + \sum_i \rho_i c_i \,, \tag{21}$$

where $\rho_0(T)$ is the temperature dependent resistivity of the pure matrix, ρ_i the resistivity of *i*-th solute element, and c_i the concentration of *i*-th element in the solution. The resistivity of pure elements suggested in the electrical property handbook are ρ_{Fe} =1.05×10^{-7} Ω·m, ρ_{Ni} =0.7×10^{-7} Ω·m, ρ_{Cr} =1.29×10^{-7} Ω·m and ρ_{Mo} =5.3×10^{-8} Ω·m. The values of electrical resistivity of elements are temperatures dependent, which are available from physical property handbook and commercial database. For the Fe-based alloy discussed in the present work, one has $\rho_0(T) = \rho_{Fe}$. The calculated electrical resistivity for matrix (ρ_m) and precipitate (ρ_p) is converted to the corresponding electrical conductivity σ_0 and σ_n via $\sigma_0 = 1/\rho_m$ and $\sigma_n = 1/\rho_n$ for the calculation of current distribution using Eq. (19). The composition of a precipitate is, in principle, dependent on its radius. This is described by Gibbs-Thomson equation [12]

$$c_i = c_i^{eq} \exp\left(2\sigma V_m / r\alpha RT\right), \tag{22}$$

where c_i^{eq} is the concentration of *i*-th element in equilibrium with a particle of infinite radius. σ is the interfacial energy, V_m is the molar volume of precipitate, r is the particle radius, α is the stoichiometric factor, *R* is the gas constant and *T* is the absolute temperature. When the particle radius is changed from r_1 to r_2, the change of solute concentration can be calculated by following approximations

$$c_i(r_2) - c_i(r_1) = c_i^{eq} \frac{2V_m\sigma}{\alpha RT}\left(\frac{1}{r_2} - \frac{1}{r_1}\right), \tag{23}$$

Table 1 Numerical results for stainless steel in electric field.

r $\times 10^{-4} m$	ρ_p $\times 10^{-7} \Omega \cdot m$	ρ_m $\times 10^{-7} \Omega \cdot m$	$\left\|\vec{j}_0(r)\right\|$ $\times 10^{9} A/m^2$	$G_j(r)/\left\|\vec{j}_0(r)\right\|^2$ $\times 10^{-17} Jm^4/A^2$
2	1.45056	1.34903	7.487350	-1.601531
4	1.39126	1.34885	7.487367	-1.601529
6	1.37556	1.34818	7.487429	-1.601524
8	1.36835	1.34722	7.487483	-1.601506
10	1.36422	1.34572	7.487543	-1.601473

One introduces 100 spherical precipitates with identical size of $r = \Delta h$ in random position initially. The changes of free energy are calculated when the precipitates grow to radiuses of $2\Delta h$, $3\Delta h$, $4\Delta h$ and $5\Delta h$ respectably. The results are presented in Table 1, where ρ_m and ρ_p are calculated by Eq. (21) with the calculated chemical compositions in matrix and precipitates. The chemical compositions in precipitate are calculated using Eq. (23). The chemical composition of matrix is calculated using mass conservation and that of volume and chemical compositions of precipitate. $\left|\vec{j}_0(r)\right|$ is the numerical calculated average current density. It can be see that the system free energy increases when the precipitates growths in a constrain of the fixed average current density $\left|\vec{j}_0(r)\right|$. In other words, the numerical calculation reveals that the electric current helps to dissolve the precipitates in stainless at high temperature annealing. The numerical results are in agreement with the experimental observation [10].

It is possible to use the method presented in the present work to calculate electric current distribution, temperature rising distribution due to Ohm heat and system free energy of

multiphase and multicomponent materials. This will help the design of electric current metallurgy from thermodynamic point of view.

Summary

1) The extra free energy caused by the electric current at steady state in linear non-dispersive materials can be calculated using $G_e = -\frac{1}{8\pi}\int_V\int_V \frac{\mu(r')\vec{j}(r')\cdot\vec{j}(r)}{|r-r'|}drdr'$. The materials may contain phases with different values of magnetic permeability.

2) In discrete model, the electric current density distribution can be calculated by $j_{\alpha\gamma} = (\phi_\alpha - \phi_\gamma)\sigma_{\alpha\gamma}/S_{\alpha\gamma}$, where the electrical potential distribution can be calculated numerically using relaxation method using $\phi_\alpha = \sum_{\gamma=1}^{\beta}\phi_\gamma\sigma_{\alpha\gamma}/\sum_{\gamma=1}^{\beta}\sigma_{\alpha\gamma}$. The method is suitable for the low-frequency limit. The latter is valid for most engineering metallurgical processing.
3) The heating rate caused by Ohm heat can be calculated using the equation of $\dot{T}_{\alpha\gamma} = (\phi_\gamma - \phi_\alpha)^2\sigma_{\alpha\gamma}/(m_{\alpha\gamma}c_{\alpha\gamma})$ in discrete simulation. The percolation effect in multiphase materials has been included.
4) The validity of the method presented in the present work has been examined against the analytical solution. The numerical results are in agreement with experimental observations in the precipitation behaviour in multicomponent alloys.

Acknowledgements

RQ is grateful to TATA Steel and the Royal Academy of Engineering for the sponsorship of the Senior Research Fellowship.

References

1. R. S. Qin: ‘Outstanding issues in electropulsing processing’, *Mater. Sci. Technol.*, 2015, **31**, 203-206.
2. O.Redlich and A.T. Kister: ‘Algebraic representation of thermodynamic properties and the classification of solutions’, *Ind. Eng. Chem.*, 1948, **40**, 345-349.
3. Y. K. Luo and R. S. Qin: ‘Surface energy and its anisotropy of hexagonal close-packed metals’, Surf. Sci., 2014, **630**, 195–201.
4. J. D. Eshelby; ‘The determination of the elastic field of an ellipsoidal inclusion, and related problems’, *Proc. R. Soc. London A*, 1957, **241**, 376-396.
5. Y. Dolinsky and T. Elperin: ‘Thermodynamics of nucleation in current-carrying conductors’, *Phys. Rev. B*, 1994, **50**, 52–58.
6. R. S. Qin and B. L. Zhou: ‘Effect of electric current pulses on grain size in castings’ *Int. J. Non-Equilib. Proc.*, 1998, **11**, 77-86.
7. R.S. Qin and S.X. Su, ‘Thermodynamics of crack healing under electropulsing’ *J. Mater. Res.*, 2002, **17**, 2048-2052.
8. R. S. Qin, E. I. Samuel and A. Bhowmik: ‘Electropulse-induced cementite nanoparticle formation in deformed pearlitic steels’, *J. Mater. Sci.*, 2011, **46**, 2838–2842.
9. D. Leenov and A. Kolin: ‘Theory of electromagnetophoresis. I. magnetohydrodynamic forces experienced by spherical and symmetrically oriented cylindrical particles, *J. Chem. Phys.*, 1954, **22**, 683-688.
10. R. S. Qin, A. Rahnama, W. J. Lu, X. F. Zhang and B. Elliott-Bowman: ‘Electropulsed steels’, *Mater. Sci. Technol.*, 2014, **30**, 1040-1044.
11. P. Guyot and L. Cottignies: ‘Precipitation kinetics, mechanical strength and electrical conductivity of AlZnMgCu alloys’, *Acta Mater.*, 1996, 44, 4161-4167.
12. D. H. Bratland, Ø. Grong, H. Shercliff, O. R. Myhr, S. Tjøtta, ‘Modelling of precipitation reactions in industrial processing’, *Acta Mater*. 1997, *45*, 1-22.